IEEE Access
Multidisciplinary | Rapid Review | Open Access Journal

Received November 10, 2017, accepted January 30, 2018, date of publication February 5, 2018, date of current version March 16, 2018.

Digital Object Identifier 10.1109/ACCESS.2018.2802481

Research on the Parameter Optimization of Electronic Ballast for UV-Lamps Considering Its Lifetime and UVC Irradiance

XIANGJUN ZHANG[1,2], KOUJIE DONG[1,2], YIJIE WANG[2], (Senior Member, IEEE), DIANGUO XU[2], (Fellow, IEEE), AND JIN JIANG[1]

[1]Department of State Key Laboratory of Urban Water Resource and Environment, Harbin Institute of Technology, Harbin 150090, China
[2]Department of Electrical Engineering, Harbin Institute of Technology, Harbin 150001, China

Corresponding author: Xiangjun Zhang (xiangjunzh@hit.edu.cn)

This work was supported in part by the Open Project of State Key Laboratory of Urban Water Resource and Environment, Harbin Institute of Technology, under Grant QAK201505, in part by the National Natural Science Foundation of China under Grant 51577042, and in part by the National High Technology Research and Development Program 863 of China under Grant 2015AA050603.

ABSTRACT To enhance the UVC irradiation and prolong the life span of UV-lamps, parameter optimization is conducted for electronic ballasts. In this paper, the double capacitor topology is adopted and the effects of different ratios of shunt capacitors are investigated. Experiments are performed under different lamp power levels for each shunt capacitor ratio. The irradiance in each waveband emitted by the UV-lamp is measured using illuminometers and the variation trends are studied based on the excitation characteristics of mercury atoms. The effective lifetime of the UV-lamp is obtained through application tests, and it is verified to be remarkably prolonged when the double capacitor topology is adopted. Analyses and comparisons are discussed and an optimum shunt capacitor ratio is obtained, taking both increasing the UVC irradiation and prolonging the lifetime of the lamp into consideration.

INDEX TERMS Electronic ballast, parameter optimization, ultraviolet sources, irradiance, lifetime.

I. INTRODUCTION

Ultraviolet (UV) disinfection, a highly efficient disinfection method that does not produce any harmful by-products, has gradually become the most reliable method of sewage treatment [1]–[3]. UV radiation produced by a UV-lamp includes UVA (320–400 nm), UVB (280–320 nm), UVC (200–280 nm), and VUV (100–200 nm), as shown in Fig. 1. Only UVC can perform microbial inactivation and organic degradation, which is favorable for sewage treatment [4]. Therefore, studying how to increase the UVC irradiance under the same power level is important. The expected lifetime of the UV-lamp should also be considered.

The research performed on fluorescent lamps, which are the same as UV lamps except the latter do not contain phosphor, has made significant progress. High frequency electronic ballasts have become the preferred drive circuits for fluorescent lamps and UV-lamps due to their small size, energy saving capability, and high stability [5]–[9]. To prolong lamp life, F. T. Wakabayashi presented a methodology for the adjustment of the preheating process and steady-state operation of electronic ballasts intended for hot-cathode fluorescent lamps. The preheating process was based on the imposition of a constant RMS current through the electrodes in order to provide a proper value of the R_h/R_c ratio before the lamp starts [10], [11]. The effect of preheating time on the filament temperature and the life span of the lamp was studied in [12].

For solving the issue of drinking water purification, Arenas *et al.* presented a design methodology for electronic ballasts applied to UV-lamps that provided an adjustable UV dose in order to ensure the inactivation of microorganisms' reproduction in [13]. A high efficiency fluorescent lamp electronic ballast was proposed in [6] by implementing a series resonant inverter in a half-bridge configuration instead of the classic series–parallel resonant inverter. However, it did not consider the effective UVC irradiance. The efficiency of the voltage-fed half-bridge resonant inverter was higher than that of the current-fed push-pull resonant inverter [14].

Much research has been conducted to explore how the fluorescent lamp interacts with the ballast. Power and voltage models of the electrode were derived under certain

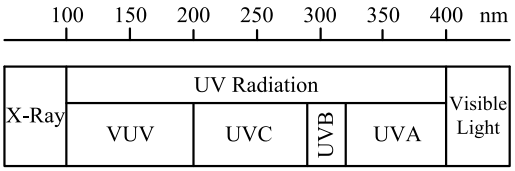

FIGURE 1. UV radiation spectrum.

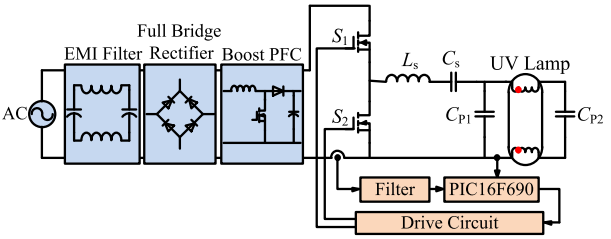

FIGURE 2. High frequency electronic ballast topology of the UV-lamp.

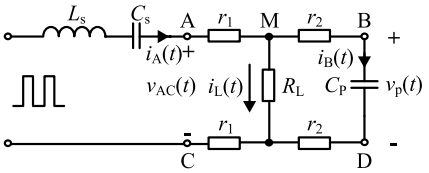

FIGURE 3. LCC series-parallel resonant circuit with a single parallel resonant capacitor C_p.

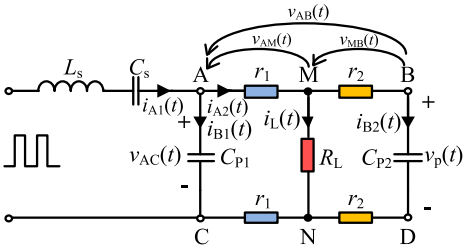

FIGURE 4. Improved LCC series-parallel resonant circuit.

conditions in [15], and a method that combines DC bus voltage regulation with switching frequency regulation to control the electrode power was proposed based on the voltage model. By controlling the electrode power, the electrode can provide moderate thermionic emission under different lamp power levels, thereby prolonging the service life of the fluorescent lamp. Reference [16] presented a performance comparison between DC bus voltage and inverter frequency variation dimming methods for the electronic ballast used to drive a T5 28 W fluorescent lamp. The Simulink simulation of a dynamic conductance-based wattage-independent compact fluorescent lamp model in a high frequency environment was presented in [17]. The model coefficients were replaced by four polynomial equations derived from experimental data.

Another solution often employed to study the lamp-ballast interaction is to obtain the small-signal incremental impedance and the ballast output impedance of the lamp in order to investigate the stability of the system. In [18], a single-pole single-zero transfer function was proposed and researched to approximate the lamp small-single impedance and the small-signal model parameters were obtained as a function of the lamp power. However, the accuracy of the single-pole single-zero model was significantly reduced for dimmable circuits at relatively low power levels. To improve the performance at low power, a power-dependent small-signal model based on a double-complex-pole double-real-zero approximation for fluorescent lamps was presented in [19] and [20]. Although it is more accurate than the single-pole single-zero model under low-power conditions, this method is more complex and difficult to calculate and is only used to estimate the stability of the lamp. Reference [21] examined the effects of lamp temperature on small-signal characteristics of fluorescent lamps.

To investigate the characteristic of excitation of mercury atoms, a fluorescent lamp model based on its physical properties was proposed in [22]. In [23] and [24], a collisional-radiative model was proposed by Loo *et al.*. It can describe in detail the microscopic reactions in a discharge according to three sets of continuity equations: particle balance, electron energy, and gas temperature. Although this is a good method to model the electrical behavior of the lamp in a ballast environment, it is not easy for manufacturers to readily accept the sophisticated calculation and abstract analysis. In addition, the study did not directly determine how to optimize the design of electronic ballasts in order to improve the UVC irradiance, especially at higher lamp power levels.

In this study, the main topology adopted is the half-bridge LCC resonant circuit, which was presented in [25]. A proper filament preheating current, an adequate starting voltage, and an AC voltage with appropriate amplitude in a stable state are provided to ensure the reliability and efficiency of the circuit. To enhance the UVC irradiation and prolong the life span of the UV-lamp, a parameter optimization is conducted for the electronic ballast and the double capacitor topology is adopted as an improvement. Experiments are performed and the effects of different ratios of shunt capacitors are investigated. Analyses and comparisons are studied based on theoretical and experimental results to prove the superiority of the topology.

II. THEORETICAL BASIS OF THE UV-LAMP

A. THEORETICAL ANALYSES OF THE ELECTRONIC BALLAST

The block diagram of the high frequency electronic ballast topology adopted in this paper for the UV-lamp is shown in Fig. 2. The LCC series-parallel resonant circuit with a single parallel resonant capacitor C_p was often used, as shown in Fig. 3. Different from the single capacitor circuit presented in [25], the proposed LCC series-parallel resonant topology adopts the double capacitor structure to enhance the UVC irradiation and prolong the life span of UV-lamps. Fig. 4 shows the improved LCC series-parallel resonant circuit and the corresponding resistance model.

In Fig. 4, the relationship between the values of C_{p1} and C_{p2} is decided by (1). In addition, the value of C_p is determined by the parallel resonant frequency of the circuit,

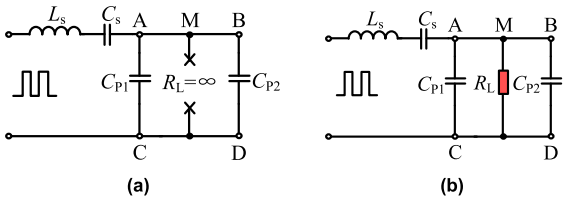

FIGURE 5. Equivalent circuits in the starting stage and the steady state. (a) During the starting stage. (b) In the steady state.

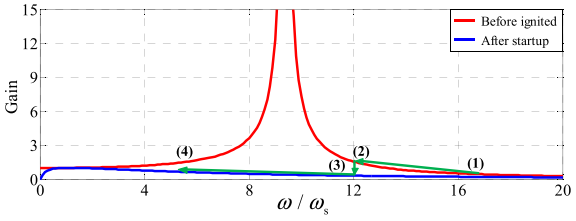

FIGURE 6. Gain–frequency characteristic curve of the LCC resonant circuit.

considering the preheating function before the lamp is ignited. The value of C_p is calculated using the method of calculation proposed in [25].

$$C_{p1} + C_{p2} = C_p \tag{1}$$

Fig. 5 shows the equivalent circuits in the starting stage and steady state, ignoring the resistances of both electrodes. The equivalent resistance of the lamp is so large in the starting stage that it is equivalent to an open-circuit load, as shown in Fig. 5 (a). In this case, C_{p1} and C_{p2} can be considered as connected in parallel. Together with L_s, they constitute a parallel resonant circuit, providing the necessary high start-up voltage through sliding frequency control.

However, the equivalent resistance of the lamp will immediately become extremely small as soon as the lamp is ignited. The series resonant circuit comprising L_s and C_s starts to dominate as shown in Fig. 5 (b), supplying power to lamp. It can be clearly seen that the adoption of the double capacitor topology has no effect on the steady state of the lamp. Besides, the existence of C_{p1} can perform a shunting action. As a result, the current stress for the lamp will be reduced effectively.

The voltage transfer characteristic of the LCC series-parallel resonant circuit can be expressed by (2).

$$H_v = \frac{V_L}{U_{in}} = \frac{1}{\sqrt{\left[1 - \left(\left(\frac{\omega}{\omega_s}\right)^2 - 1\right)\frac{C_p}{C_s}\right]^2 + Q_s^2\left[\frac{\omega}{\omega_s} - \frac{\omega_s}{\omega}\right]^2}} \tag{2}$$

where $Q_s = \omega_s L_s / R_L$ is the series quality factor and $\omega_s = 2\pi f_s$.

Based on formula (2), the gain-frequency characteristic curve of the LCC resonant circuit is obtained through MATLAB and is shown in Fig. 6. The red line represents the gain–frequency characteristic curve of the lamp before it is ignited, while the blue line shows the same curve after it is lighted. Points (1)–(4) present the process of soft starting, the same as that described in [25].

B. ANALYSES AND COMPARISONS BASED ON THE UV-LAMP

According to Fig. 4, equations (3) and (4) are easy to obtain by KCL. The RMS values of $i_{A1}(t)$, $i_{A2}(t)$, $i_{B1}(t)$, and $i_{B2}(t)$ can be directly measured through an oscilloscope but $i_L(t)$ cannot because it is the current flow through the lamp.

$$i_{A1}(t) = i_{A2}(t) + i_{B1}(t) \tag{3}$$

$$i_{A2}(t) = i_L(t) + i_{B2}(t) \tag{4}$$

In addition, according to the LCC series-parallel resonant circuit with a single parallel resonant capacitor C_p, which is shown in Fig. 3, equation (5) can be obtained by KCL.

$$i_A(t) = i_L(t) + i_B(t) \tag{5}$$

Comparing (3), (4), and (5), it can be derived that $i_{A1}(t)$ is almost the same as $i_A(t)$ under the same lamp power. Therefore, the currents that flow through the electrodes$i_{A2}(t)$ and $i_{B2}(t)$ are reduced due to the shunting action of C_{p1}.

The life expectancy of a UV-lamp mainly depends on the lifetime of the electrodes. The faster the coating material of the electrodes is lost, the shorter the life of the UV-lamp is. Since a larger starting voltage will generate more sputtering, it is necessary to provide an electrode preheating current. This current can be realized by C_{p2} in the circuit shown in Fig. 4. Additionally, a relatively larger current or voltage can cause severe sputtering in the steady state and can also reduce the lifetime of the lamp. The rate at which the filaments burn is correlated to the currents flowing through them. Reducing the currents that flow through the electrodes$i_{A2}(t)$ and $i_{B2}(t)$ is of great importance and can be realized by the shunting action of C_{p1}. The double capacitor topology is generally a good choice to extend the lifetime of the lamp.

It is important to note that the currents flowing through the electrodes should be large enough for proper preheating. Besides, too small filament current can also cause the lamp to sputter seriously, which will dramatically shorten the lifetime of the lamp. Therefore, the ratio of C_{p1} and C_{p2} should be carefully considered when their summation is a constant. In this paper, experiments are designed and carried out to obtain the optimum ratio, taking into account the preheating current, the life span, and the effective UVC irradiance generated by the lamp.

III. THEORY OF THE EXCITATION OF MERCURY ATOMS

A simplified diagram of the energy levels of the mercury atom is shown in Fig. 7. It contains the ground state 6^1S_0, and the excited states 6^1P_1, 6^3P, 6^3D, and 7^3S. The arrows pointing upward and downward in the figure represent the excitation and de-excitation processes, respectively. It is known from

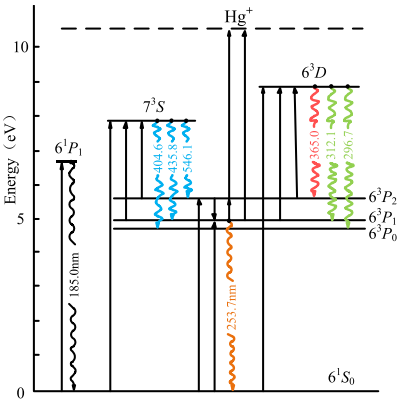

FIGURE 7. Simplified diagram of the energy levels of the mercury atom.

collision theory that electrons may produce excitation collisions with mercury atoms if they have accumulated adequate energies [22]. The mercury atoms will be excited to another excited state with a higher energy through absorbing energy from collisions with electrons. If electrons have higher energy, more mercury atoms will go through second excitation or multi-excitation. This phenomenon is more significant in lamps with higher rated power. When excited mercury atoms return to the ground state or lower energy levels, photons that possess corresponding energy are emitted. The emitted photons can be reabsorbed by the mercury atoms that stay at lower excited states. However, the probability of this occurring is extremely small since the possibility of a second excitation or multi-excitation is much smaller than that of a single excitation.

The excited mercury atoms will typically remain in one of three energy levels: 6^3P_0, 6^3P_1, and 6^3P_2, of which the excited state 6^3P_1 is the only one that can be excited from the ground state directly. The excited mercury atoms at metastable states 6^3P_0 and 6^3P_2 are common because the lifetime of excited mercury atoms at these states is quite long (up to 10^{-2}s), compared to that of other excited mercury atoms (typically 10^{-8}s). It is important to take these two metastable states into consideration while performing theoretical analysis. In high-power applications, there will be some mercury atoms that are excited to the energy levels 6^3D and 7^3S through multi-excitation. Therefore, these two levels should also be considered.

All of the lights generated by the lamp can fall into five categories: UVA, UVB, UVC, VUV, and visible light. In Fig. 7, 365.0 nm (marked by the red arrow) belongs to UVA, 312.1 nm and 296.7 nm (marked by the green arrows) are portions of UVB, 253.7 nm (marked by the brown arrow) is a part of UVC, 404.6 nm, 435.8 nm, and 546.1 nm (marked by the blue arrows) are attributed to visible light, and 185.0 nm pertains to VUV.

In order to investigate the UV irradiance at different ratios of shunt capacitors C_{p1} and C_{p2}, illuminometers will be employed to gauge the irradiance in the wavebands described

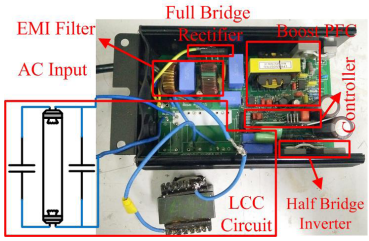

FIGURE 8. High frequency electronic ballast for the UV-lamp.

TABLE 1. Specific values of shunt capacitors at different ratios.

Groups	1	2	3	4	5	6	7
C_{p1} (nF)	0	1	2	3.3	4.4	5.6	6.6
C_{p2} (nF)	7.5	6.6	5.6	4.4	3.3	2	1
C_p (nF)	7.5	7.6	7.6	7.7	7.7	7.6	7.6

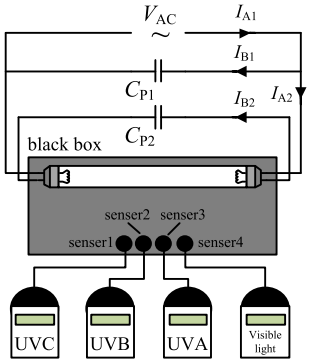

FIGURE 9. Schematic diagram of the measurement.

above except for VUV since it can only be measured in a vacuum. A good topology should increase the UVC irradiance while increasing the lifetime of the lamp under different lamp power levels. Experiments will be performed in the next section to verify the theoretical analyses above.

IV. EXPERIMENTAL RESULTS AND ANALYSIS

Fig. 8 is the physical representation of the high frequency electronic ballast for 120 W UV-lamps adopted in this study. $L_s = 967\ \mu$H, $C_s = 640$ nF, and $C_p = C_{p1} + C_{p2} = 7.5$ nF are the component values.

To verify the superiority of the double capacitor topology, experiments are performed at different ratios of shunt capacitors C_{p1} and C_{p2}. The specific values of capacitance at different ratios are listed in Table 1. The irradiance in each waveband emitted by the lamp is measured by illuminometers, as shown in Fig. 9.

Fig. 10 shows the UVC irradiance under different lamp power levels for each ratio of C_{p1} and C_{p2}. The navy-blue line represents the results when the single capacitor topology is adopted. It can be seen that the UVC irradiance is increased as C_{p2} is reduced while keeping lamp power constant. The variation trend is obtained for different lamp power levels,

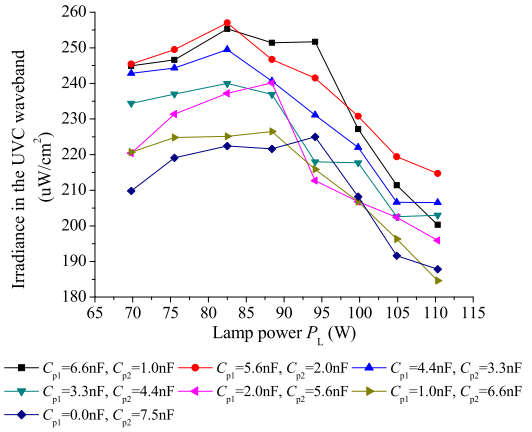

FIGURE 10. UVC irradiance under different lamp power levels for each ratio of C_{p1} and C_{p2}.

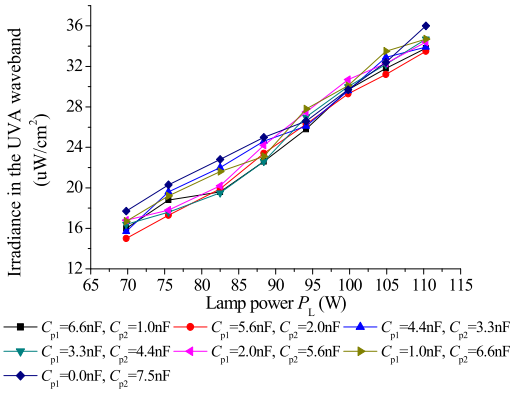

FIGURE 11. UVA irradiance under different lamp power levels for each ratio of C_{p1} and C_{p2}.

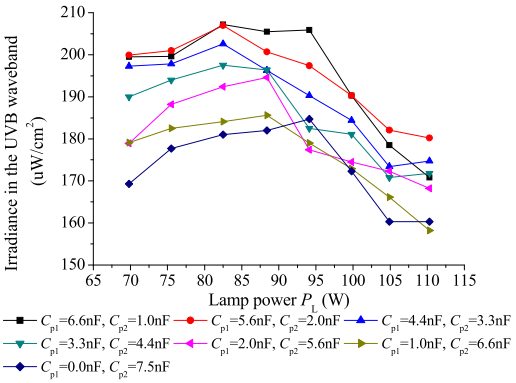

FIGURE 12. UVB irradiance under different lamp power levels for each ratio of C_{p1} and C_{p2}.

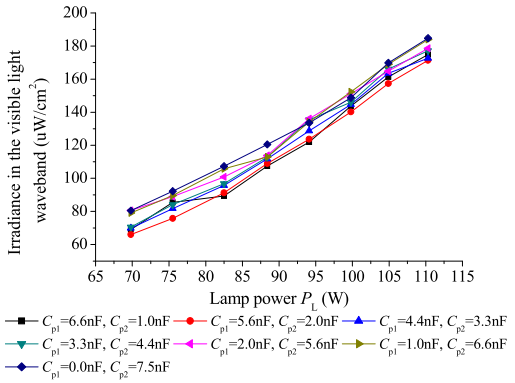

FIGURE 13. Irradiance in the visible light waveband under different lamp power levels for each ratio of C_{p1} and C_{p2}.

while ignoring unavoidable measurement errors. It can be concluded that UVC irradiance is enhanced at different lamp power levels, adopting the double capacitor topology. Moreover, the UVC radiation is more intense when the value of C_{p2} is smaller and C_{p1} is larger. Therefore, the double capacitor topology is superior for increasing the UVC irradiance.

Additionally, it can be seen from Fig. 10 that the UVC irradiance peaks are at around 82 W when the ratio of C_{p1} and C_{p2} is fixed. This can be explained by the excitation characteristics of mercury atoms. When the lamp power is low, the thermionic emission capacity of the cathode is weak because the lamp current is too small to provide sufficient temperature to permit the excitation of mercury atoms. As the lamp power becomes gradually higher, the lamp current increases as the lamp voltage decreases, which is conducive for promoting thermionic emission. The UVC radiation is enhanced because of the higher frequency collisions and excitations. However, the UVC irradiance decreases when the lamp power is larger than a certain value because the probability of second excitation and multi-excitation occurring is increased considerably.

Figs. 11–13 display the irradiance in the UVA, UVB, and visible light wavebands, respectively. As C_{p2} is reduced, the irradiance in the UVA and visible light wavebands decreases and it contributes the increases of UVC irradiance. As can be seen from Fig. 7, the generation of radiation at 312.1nm is related to the excited state 6^3P_1, so the irradiance in the UVB waveband has the same variation trend as the UVC.

It is necessary to mention that the lamp power P_L changes slightly for different ratios of C_{p1} and C_{p2}, as shown in Fig. 14. At a given lamp power set value, as the capacitance of C_{p2} decreases and C_{p1} increases, I_{B2} will be smaller and I_{B1} will be greater. This implies that the shunting action of C_{p1} is greater; thus, the currents that flow through the electrodesI_{A2} and I_{B2} are reduced and the lifetime of the lamp is extended. The thermionic emission capacity of the electrodes is weakened since the current I_L becomes smaller and the equivalent resistance of the lamp R_L becomes larger. To keep the lamp power constant, the switching frequency f_s is set higher to compensate for the effects of the change in equivalent resistance R_L. A change in frequency can considerably affect the switching loss of the MOSFETs in the half-bridge inverting circuit. A higher switching frequency will lead to a lower switching loss; as a result, the variation trend of lamp power P_L in Fig. 14 is reasonable. Additionally, the higher equivalent resistance R_L will increase the equivalent impedance at the lamp terminal; as a result, the

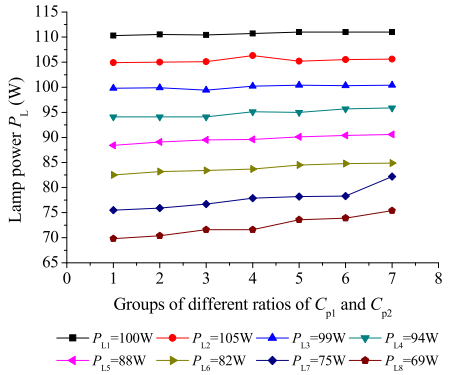

FIGURE 14. Comparison of the lamp power P_L at different ratios of C_{p1} and C_{p2}.

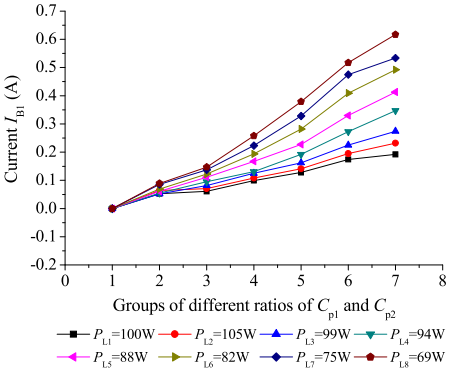

FIGURE 15. Comparison of the current I_{B1} at different ratios of C_{p1} and C_{p2}.

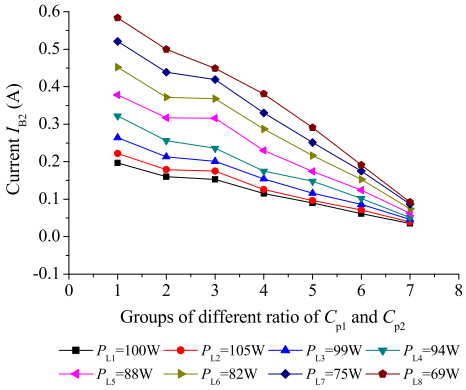

FIGURE 16. Comparison of the current I_{B2} at different ratios of C_{p1} and C_{p2}.

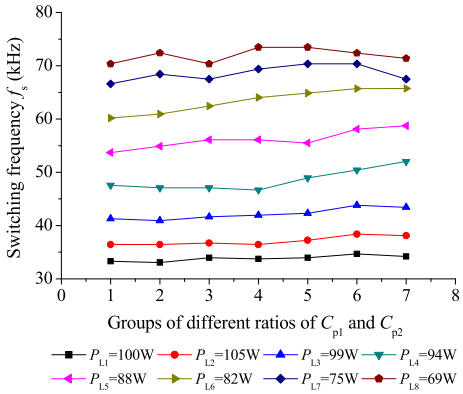

FIGURE 17. Comparison of the switching frequency f_s at different ratios of C_{p1} and C_{p2}.

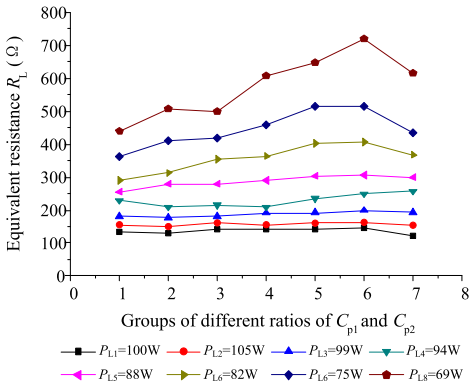

FIGURE 18. Comparison of the equivalent resistance R_L at different ratios of C_{p1} and C_{p2}.

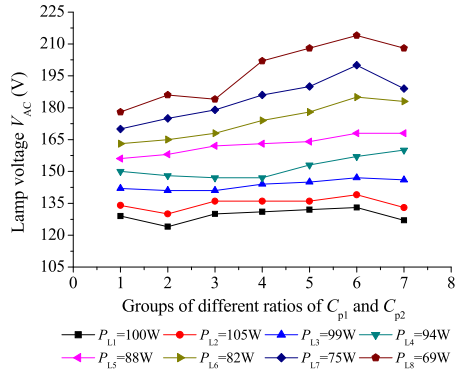

FIGURE 19. Comparison of the lamp voltage V_{AC} at different ratios of C_{p1} and C_{p2}.

lamp voltage V_{AC} will be higher and the current I_{A2} will be lower. Corresponding comparisons of the variables discussed above at different ratios of C_{p1} and C_{p2} are displayed in Figs. 15–20. The theoretical and experimental results are in good agreement.

The experimental waveforms for each ratio of C_{p1} and $C_{p2}$are shown in Figs. 21–27 with the lamp power set at 88 W. It can be seen that $v_{AC}(t)$ and $i_{A2}(t)$ have a slight variation, while $i_{B1}(t)$ and $i_{B2}(t)$ vary significantly with the ratio of C_{p1} and C_{p2} as discussed earlier.

Considering the preheating function of C_{p2}, the value of i_{B2} cannot be too small. In addition, the strong shunting capability of C_{p1} will lead to extremely small lamp current, which will reduce the life time of the lamp. On balance, choose C_{p1} to be 5.6 nF and C_{p2} to be 2 nF that is, $C_{p2}/C_{p1} = 0.36$ is considered to be the best ratio to enhance UVC irradiance and prolong the lifetime of the lamp for 120 W UV-lamps. Besides, experiments for lamps with rated power of 72 W and

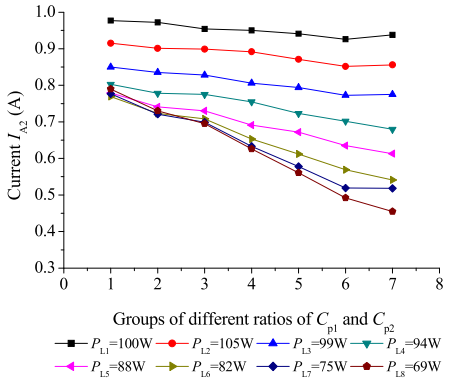

FIGURE 20. Comparison of the current I_{A2} at different ratios of C_{p1} and C_{p2}.

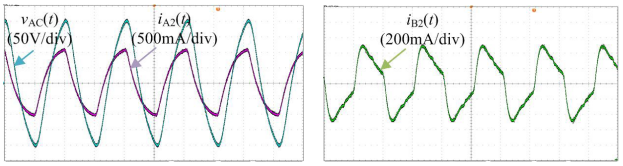

FIGURE 21. Experimental waveforms when $C_{p1} = 0$ nF and $C_{p2} = 7.5$ nF. (a) Lamp voltage v_{AC} (t) and current i_{A2} (t). (b) Current i_{B2} (t).

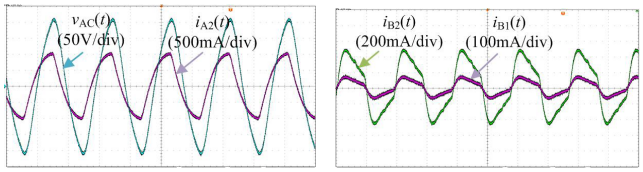

FIGURE 22. Experimental waveforms when $C_{p1} = 1$ nF and $C_{p2} = 6.8$ nF. (a) Lamp voltage v_{AC} (t) and current i_{A2} (t). (b) Current i_{B1} (t) and i_{B2} (t).

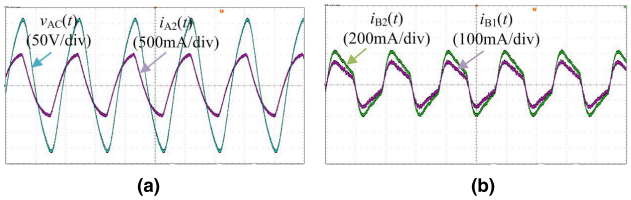

FIGURE 23. Experimental waveforms when $C_{p1} = 2$ nF and $C_{p2} = 5.6$ nF. (a) Lamp voltage v_{AC} (t) and current i_{A2} (t). (b) Current i_{B1} (t) and i_{B2} (t).

36 W are carried out, using the parameter optimization model presented above. $C_{p2}/C_{p1} = 0.30$ and 0.25 are obtained as the best ratios at around 50W and 28W respectively. Thus, in general, $C_{p2}/C_{p1} = 0.30$ can be considered to be the best ratio for UV-lamps with different rated power to enhance the UVC irradiance and prolong the lifetime of the lamp.

To verify that the lifetime of the lamp is prolonged by adopting the optimization scheme discussed above, application tests are conducted by the partner Daqing Qingyuan Water Treatment Technology Co., Ltd. In the condition the single capacitor topology ($C_p = 7.5$ nF) is applied, the

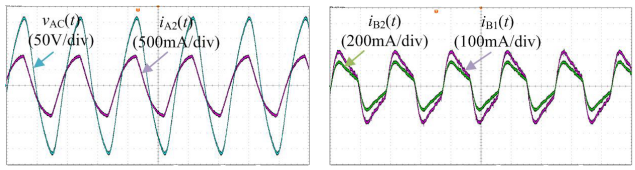

FIGURE 24. Experimental waveforms when $C_{p1} = 3.3$ nF and $C_{p2} = 4.4$ nF. (a) Lamp voltage v_{AC} (t) and current i_{A2} (t). (b) Current i_{B1} (t) and i_{B2} (t).

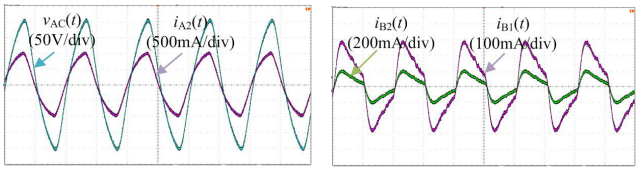

FIGURE 25. Experimental waveforms when $C_{p1} = 4.4$ nF and $C_{p2} = 3.3$ nF. (a) Lamp voltage v_{AC} (t) and current i_{A2} (t). (b) Current i_{B1} (t) and i_{B2} (t).

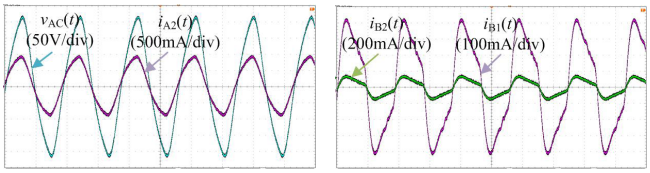

FIGURE 26. Experimental waveforms when $C_{p1} = 5.6$ nF and $C_{p2} = 2$ nF. (a) Lamp voltage v_{AC} (t) and current i_{A2} (t). (b) Current i_{B1} (t) and i_{B2} (t).

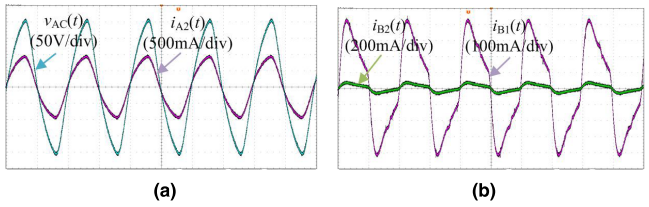

FIGURE 27. Experimental waveforms when $C_{p1} = 6.6$ nF and $C_{p2} = 1$ nF. (a) Lamp voltage v_{AC} (t) and current i_{A2} (t). (b) Current i_{B1} (t) and i_{B2} (t).

effective lifetime of the T5 120 W UV-lamp is only 41 days at $P_L = 110$ W and 92 days at $P_L = 88$ W. However, the lamp with the same rated power can last for 96 days at $P_L = 110$ W and 230 days at $P_L = 88$ W when the double capacitor topology ($C_{p2}/C_{p1} = 0.30$) is adopted. As can be seen from the results, the life span of the lamp increases more than two times when using the optimization scheme presented above. It can be concluded that the optimization scheme proposed in this paper prolongs the lifetime of the lamp remarkably.

V. CONCLUSION

In this study, parameter optimization is investigated for electronic ballasts and the double capacitor topology is adopted to increase the UVC irradiation and prolong the lifetime of the UV-lamp. Experiments are performed under

different lamp power levels with different ratios of C_{p1} and C_{p2}. The irradiance in each waveband emitted by the UV-lamp is measured with illuminometers, which verifies that the UVC irradiation is enhanced considerably for different lamp power levels. The lifetime of the lamp is remarkably prolonged since the currents that flow through the electrodes are reduced, which is verified by application tests. An optimum ratio of $C_{p2}/C_{p1} = 0.30$ for UV-lamps with different rated power is obtained by considering both increasing the UVC irradiation and prolonging the lifetime of the UV-lamp. This study has great significance for sewage treatment applications by raising the efficiency of UVC radiation and the lifespan of UV-lamps.

REFERENCES

[1] M. G. Raizen, "Mercury isotopes for efficient uv lamps and fluorescent lighting," *IEEE Trans. Ind. Appl.*, vol. 52, no. 6, pp. 5231–5234, Nov./Dec. 2016.
[2] M. Ben Mustapha and H. Abdnnaceur, "Modeling and performance improvement of a method for the disinfection of water by UV irradiation as a function of the power of the low pressure lamp discharge mode," in *Proc. Int. Conf. Elect. Sci. Technol. Maghreb (CISTEM)*, Tunis, Tunisia, 2014, pp. 1–8.
[3] J. Hong and M. Otaki, "Studies on liposome-encapsulated-chemical actinometer in UV-disinfection by low pressure UV lamp: Bio-chemical actinometer in UV-disinfection," in *Proc. Int. Conf. Biomed. Eng. Biotechnol.*, Macao, China, 2012, pp. 1704–1707.
[4] U. S. Osman and A. F. Omar, "Solar ultraviolet measurement: A mini review," in *Proc. Int. Conf. Adv. Elect., Electron. Syst. Eng. (ICAEES)*, Putrajaya, Malaysia, Nov. 2016, pp. 252–257.
[5] S.-Y. Chan, T.-H. Yang, and Y.-N. Chang, "Design of electronic ballast for short-arc xenon lamp with interleaved half-wave rectifier," *IEEE Trans. Power Electron.*, vol. 31, no. 7, pp. 5102–5112, Jul. 2016.
[6] J. F. Bayona, H. R. Chamorro, A. C. Sanchez, D. A. Rubio, and J. Aguillon-Garcia, "A high efficiency fluorescent lamp electronic ballast design," in *Proc. IEEE Conf. Comput. Sci. (CACIDI)*, Buenos Aires, Argentina, Nov./Dec. 2016, pp. 1–4.
[7] K. Chen, P. Xiao, A. Johnsen, and R. E. Saenz, "Turn-on optimization for class D series-parallel LCC-type constant current high-power led driver design based on traditional fluorescent control IC," *IEEE Trans. Power Electron.*, vol. 31, no. 7, pp. 4732–4741, Jul. 2016.
[8] M. F. Menke, "Comparative analysis of self-oscillating electronic ballast dimming methods with power factor correction for fluorescent lamps," *IEEE Trans. Ind. Appl.*, vol. 51, no. 1, pp. 770–782, Jan./Feb. 2015.
[9] Y. Wang, X. Zhang, and D. Xu, "Electronic ballast for 119 W UV lamp controlled by microprocessor," in *Proc. IEEE Ind. Appl. Soc. Annu. Meeting*, Houston, TX, USA, Oct. 2009, pp. 1–5.
[10] F. T. Wakabayashi, C. S. Ferreira, M. A. G. D. Brito, and C. A. Canesin, "Model for electrodes' filaments of hot cathode fluorescent lamps, during preheating with constant RMS current," *IEEE Trans. Power Electron.*, vol. 22, no. 3, pp. 719–726, May 2007.
[11] F. T. Wakabayashi, M. A. G. D. Brito, C. S. Ferreira, and C. A. Canesin, "Setting the preheating and steady-state operation of electronic ballasts, considering electrodes of hot-cathode fluorescent lamps," *IEEE Trans. Power Electron.*, vol. 22, no. 3, pp. 899–911, May 2007.
[12] A. Mukherjee and A. Soni, "Parameters affecting the switching life in HPF self ballasted lamps," in *Proc. IEEE 1st Int. Conf. Control, Meas. Instrum. (CMI)*, Kolkata, India, Jan. 2016, pp. 103–106.
[13] L. De Oro Arenas, G. E. de Azevedo e Melo, and C. A. Canesin, "Electronic ballast design for UV lamps based on UV dose, applied to drinking water purifier," *IEEE Trans. Ind. Electron.*, vol. 63, no. 8, pp. 4816–4825, Aug. 2016.
[14] Y.-R. Yang, "Comparison of push-pull and half-bridge resonant inverters for cold cathode fluorescent lamps," in *Proc. IEEE 11th Int. Conf. Power Electron. Drive Syst.*, Sydney, NSW, Australia, Jun. 2015, pp. 696–702.
[15] S. T. S. Lee, H. S. H. Chung, and S. Y. Hui, "A novel electrode power profiler for dimmable ballasts using DC link voltage and switching frequency controls," *IEEE Trans. Power Electron.*, vol. 19, no. 3, pp. 847–853, May 2004.
[16] P. Reginatto, M. F. da Silva, R. V. Tambara, Á. R. Seidel, M. Polonskii, and J. M. Alonso, "Performance evaluation of dimmable electronic ballast based on frequency and bus voltage variation," in *Proc. 12th IEEE Int. Conf. Ind. Appl. (INDUSCON)*, Curitiba, Brazil, Nov. 2016, pp. 1–8.
[17] B. G. Bakshi and B. Roy, "Development and simulation of dynamic conductance based wattage-independent compact fluorescent lamp model in high frequency environment," in *Proc. 2nd Int. Conf. Control, Instrum., Energy Commun. (CIEC)*, Kolkata, India, Jan. 2016, pp. 225–229.
[18] R. E. Diaz, J. Ribas, A. J. Calleja, J. Garcia-Garcia, and J. M. Alonso, "Small signal characterization of fluorescent lamps in dimmed operation," in *Proc. 35th Annu. Conf. IEEE Ind. Electron.*, Porto, Portugal, Nov. 2009, pp. 3563–3568.
[19] J. Ribas *et al.*, "Using a power-dependent small-signal model for stability analysis in resonant dimming ballasts for fluorescent lamps," in *Proc. 37th Annu. Conf. IEEE Ind. Electron. Soc. (IECON)*, Melbourne, VIC, Australia, Nov. 2011, pp. 2969–2975.
[20] R. E. Diaz, J. Ribas, A. J. Calleja, J. García, D. Gacio, and M. Rico-Secades, "Power-dependent small-signal model for fluorescent lamps based on a double-pole double-zero transfer function," *IEEE Trans. Ind. Appl.*, vol. 49, no. 1, pp. 341–347, Jan./Feb. 2013.
[21] J. Ribas, R. E. Diaz, A. J. Calleja, E. Lopez-Corominas, J. Cardesín, and J. García, "Temperature effects on the small-signal characteristics of fluorescent lamps," in *Proc. 38th Annu. Conf. IEEE Ind. Electron. Soc. (IECON)*, Montreal, QC, Canada, Oct. 2012, pp. 4604–4610.
[22] M. Chen and Z. Qian, "A fluorescent lamp model based on its physical characteristics," in *Proc. 5th Int. Conf. Power Electron. Drive Syst. (PEDS)*, vol. 2. 2003, pp. 1132–1136.
[23] K. H. Loo, G. J. Moss, R. C. Tozer, D. A. Stone, M. Jinno, and R. Devonshire, "A dynamic collisional-radiative model of a low-pressure mercury-argon discharge lamp: A physical approach to modeling fluorescent lamps for circuit simulations," *IEEE Trans. Power Electron.*, vol. 19, no. 4, pp. 1117–1129, Jul. 2004.
[24] M. Ben Mustapha, B. Mrabet, L. Bouslimi, M. Stambouli, and A. Chammam, "Effect of a pulsed power supply on the ultra violet radiation and electrical characteristics of low pressure mercury discharge," in *Proc. 3rd Int. Design Test Workshop*, Monastir, Tunisia, 2008, pp. 319–324.
[25] X. Zhang, J. Zhao, and H. Yang, "The design of electronics ballast for long service life UV lamps," in *Proc. IEEE 2nd Int. Future Energy Electron. Conf. (IFEEC)*, Taipei, Taiwan, Nov. 2015, pp. 1–5.

XIANGJUN ZHANG was born in Shandong Province, China, in 1971. He received the B.S. degree in welding from Xi'an Jiaotong University, Xi'an, China, in 1993, the M.S. degree in welding from the Harbin Welding Institute, Harbin, China, in 1999, and the Ph.D. degree in electrical engineering from the Harbin Institute of Technology, Harbin, in 2006. From 2006 to 2013, he was a Lecturer with the Department of Electrical and Electronics Engineering, Harbin Institute of Technology, where he has been an Associate Professor since 2013. His research interests include the areas of electronic ballast, power factor correction circuits, high-power converters, and light emitting diode lighting systems.

KOUJIE DONG received the B.S. degree in electrical engineering from the School of Electrical Engineering & Automation, Harbin Institute of Technology, Harbin, China, in 2016. She is currently pursuing the M.S. degree in electrical engineering with the Harbin Institute of Technology. Her current research interests include the areas of electronic ballast, power factor correction circuits, and light emitting diode lighting systems.

YIJIE WANG was born in Heilongjiang, China, in 1982. He received the B.S., M.S., and Ph.D. degrees in electrical engineering from the Harbin Institute of Technology, China, in 2005, 2007, and 2012, respectively. From 2012 to 2014, he was a Lecturer with the Department of Electrical and Electronics Engineering, Harbin Institute of Technology, where he has been an Associate Professor since 2015. His interests include dc-dc converters, soft-switching power converters, power factor correction circuits, digital control electronic ballasts, LED lighting systems. He is an Associate Editor of the IEEE TRANSACTIONS ON INDUSTRIAL ELECTRONICS, *IET Power Electronics*, and *Journal of Power Electronics*.

DIANGUO XU (F'17) received the B.S. degree in control engineering from Harbin Engineering University, Harbin, China, in 1982, and the M.S. and Ph.D. degrees in electrical engineering from the Harbin Institute of Technology (HIT), Harbin, China, in 1984 and 1989, respectively. In 1984, he joined the Department of Electrical Engineering, HIT, as an Assistant Professor, where he has been a Professor since 1994. From 2000 to 2010, he was the Dean of School of Electrical Engineering and Automation, HIT. He is currently the Vice President of HIT. His research interests include renewable energy generation technology, power quality mitigation, sensorless vector controlled motor drives, and high-performance permanent magnet synchronous motor servo system. He has published over 600 technical papers.

Dr. Xu serves as the Chairman of the IEEE Harbin Section. He is an Associate Editor of the IEEE TRANSACTIONS ON INDUSTRIAL ELECTRONICS, the IEEE TRANSACTIONS ON POWER ELECTRONICS, and the IEEE JOURNAL OF EMERGING AND SELECTED TOPICS IN POWER ELECTRONICS.

JIN JIANG received the B.S., M.S., and Ph.D. degrees in environmental engineering from the Harbin Institute of Technology (HIT), China, in 2002, 2005, and 2009, respectively. He is currently a Professor with the School of Environment, HIT. His research interests mainly include the treatment of drinking water and wastewater by advanced oxidation and reduction technologies, such as UV-based photocatalysis.